An *ab Initio* Quantum Chemical Investigation of Carbon-13 NMR Shielding Tensors in Glycine, Alanine, Valine, Isoleucine, Serine, and Threonine: Comparisons between Helical and Sheet Tensors, and the Effects of χ_1 on Shielding†

Robert H. Havlin,¶,‡ Hongbiao Le,§ David D. Laws,‡ Angel C. deDios,# and Eric Oldfield*

Contribution from the Department of Chemistry, University of Illinois at Urbana−Champaign, 600 South Mathews Avenue, Urbana, Illinois 61801

Received June 2, 1997. Revised Manuscript Received September 9, 1997⊗

Abstract: The carbon-13 nuclear magnetic resonance shielding surfaces for the isotropic and anisotropic shielding components, σ_{11}, σ_{22}, and σ_{33}, for C^α in *N*-formylglycine amide, and C^α and C^β in *N*-formylalanine amide, *N*-formylvaline amide ($\chi_1 = 180°, -60°, 60°$), *N*-formylisoleucine amide (all $\chi_1 = -60°$ conformers), N-formyl serine amide ($\chi_1 = 74.3°$), and *N*-formylthreonine amide ($\chi_1 = 180°, -60°, 60°$) have been computed at the Hartree−Fock level by using large, locally dense basis sets. The results for C^α in glycine and alanine show the expected ∼4−5 ppm increase in isotropic shielding of sheet over helical geometries, and the overall breadths of the shielding tensors are very similar for both helical and sheet fragments ($|\sigma_{33} - \sigma_{11}| \sim 31-37$ ppm). However, for each of the C^β substituted amino acids (valine, isoleucine, serine, and threonine) our results for C^α indicate not only the expected ∼4−5 ppm increase in shielding of sheet fragments over helical ones but also a large increase in the overall tensor breadths for sheet residues over helical ones, and a change in tensor orientation. On average, the sheet residues have $|\sigma_{33} - \sigma_{11}| \sim 34$ ppm, while on average the helical value is only ∼22 ppm. For each C^β substituted amino acid, the results for C^α also show that $|\sigma_{22} - \sigma_{11}|$(sheet) $\gg |\sigma_{22} - \sigma_{11}|$(helix). For C^β, the helical and sheet tensor breadths are in general much more similar for a given amino acid, although the actual magnitudes vary widely from one amino acid to another. Since the individual C^α tensor elements, σ_{11}, σ_{22}, and σ_{33}, are all quite sensitive to not only the backbone torsion angles, ϕ, ψ, but also to the side chain torsion angle, χ_1, as well, these results suggest that it will in many instances be possible to deduce both backbone (ϕ,ψ) and side chain (χ_1) torsion angles from an experimental determination of the three principal elements of the $^{13}C^\alpha$ shielding tensor, results which can be confirmed in some cases with data on C^β (and C^γ). Such an approach, based on quantum chemical calculations, should be useful in determining the structures of both crystalline, noncrystalline, and potentially even soluble peptides and proteins, as well as in refining their structures, using shielding tensor elements.

Introduction

Recent improvements in *ab initio* quantum chemical methodologies, when combined with similar improvements in computer hardware, have recently permitted the first successful predictions of the ^{13}C, ^{15}N, and ^{19}F nuclear magnetic resonance spectra of proteins in solution,[1,2] and have led to methods for refining existing solution structures.[3] However, there has been relatively little attention paid to the anisotropic components of the chemical shift. This is because there is a dearth of solid-state chemical shift information available on proteins. This situation can be expected to improve as higher field spectrometers and novel multidimensional experiments are developed, and indeed there are already several examples of the determination of single-atom shifts and shielding tensor elements in quite large proteins.[4−6] It is thus timely to consider just what one might learn from an analysis of, say, a C^α or a C^β shielding tensor in a protein. Toward this end, the C^α shielding tensors in a series of alanine-containing tripeptides, e.g. ala-*ala-ala, have recently been investigated.[7] The basic idea is to use quantum chemically calculated C^α shielding surfaces[8] together with Bayesian probability[9] —the "Z-surface" method described previously for *solution* ^{13}C chemical shifts[10] —to deduce the peptide backbone torsion angles, ϕ and ψ.[7] The method has recently been shown to be quite accurate, with only small errors from X-ray crystallographic results being obtained.[7]

† This work was supported by the United States Public Health Service (National Institutes of General Medical Sciences grant GM-50694).

¶ Barry Goldwater Fellow.

‡ Present address: Department of Chemistry, University of California, Berkeley.

§ Present address: Laboratorium für Physicalische Chemie, ETH, Universitatstrasse 22, 8092, Zürich, Switzerland.

Present address: Department of Chemistry, Georgetown University, Washington, DC.

⊗ Abstract published in *Advance ACS Abstracts,* November 15, 1997.

(1) de Dios, A. C.; Oldfield, E. *Solid State NMR* **1996**, *6*, 101−126.

(2) Oldfield, E. *J. Biomol. NMR* **1995**, *5*, 217−225.

(3) Pearson, J. G.; Wang, J.-F.; Markley, J. L.; Le, H.; Oldfield, E. *J. Am. Chem. Soc.* **1995**, *117*, 8823−8829.

(4) Cole, H. B. R.; Sparks, S. W.; Torchia, D. A. *Proc. Natl. Acad. Sci. U.S.A.* **1988**, *85*, 6362−6365.

(5) Cole, H. B. R.; Torchia, D. A. *Chem. Phys.* **1991**, *158*, 271−281.

(6) Gerothanassis, I. P.; Momenteau, M.; Hawkes, G. E.; Barrie, P. J. *J. Am. Chem. Soc.* **1993**, *115*, 9796−9797. Barrie, P. J.; Gerothanassis, I. P.; Momenteau, M.; Hawkes, G. E. *J. Magn. Reson, Ser. B* **1995**, *108*, 185−188.

(7) Heller, J.; Laws, D. D.; King, D. S.; Wemmer, D. E.; Pines, A.; Havlin, R. H.; Oldfield, E., *J. Am. Chem. Soc.* **1997**, *119*, 7827−7831.

(8) de Dios, A. C.; Pearson, J. G.; Oldfield, E. *J. Am. Chem. Soc.* **1993**, *115*, 9768−9773.

(9) Box, G. E. P.; Tiao, G. C. *Bayesian Inference in Statistical Analysis*; Wiley-Interscience: New York, 1992.

(10) Le, H.; Pearson, J. G.; de Dios, A. C.; Oldfield, E. *J. Am. Chem. Soc.* **1995**, *117*, 3800−3807.

S0002-7863(97)01796-4 CCC: $14.00

The next step is to investigate the effects of side chain (χ_1) torsion angles on shielding, or more specifically, how the individual shielding tensor elements vary with ϕ,ψ and χ. Here, we will not discuss full shielding hypersurfaces, since in separate work involving geometry optimization,[11] it appears that the standard χ conformers cover most structural situations. We therefore discuss here results describing how the individual components of the C^α and C^β shielding tensors vary with ϕ,ψ at the popular χ_1 and χ_2 geometries. Full Ramachandran ϕ,ψ shielding surfaces have been computed for isoleucine, serine, and threonine at selected χ_1, χ_2 geometries, and these results are compared with full shielding tensor surfaces for glycine, alanine, and valine, whose isotropic shifts were already reported previously by us in large basis set calculations.[8] We find rather unexpected, major differences in shielding anisotropy, and asymmetry, between C^α in helical and sheet geometries in the C^β-substituted amino acids (valine, isoleucine, serine, threonine) investigated. For C^β, the differences are much smaller, and vary from one amino acid to another. These results should facilitate the further development of novel methods for structure prediction and refinement, based on the experimental determination of the principal elements of the chemical shielding tensor, both in the solid state and potentially in solution as well.[12]

Computational Details

The principal elements of the $^{13}C^\alpha$ and $^{13}C^\beta$ chemical shielding tensors, and their orientations, were computed with the Texas program[13,14] which was kindly provided by Professors Peter Pulay and James Hinton and Dr. K. Wolinski. Calculations were carried out on a cluster of International Business Machines (Austin, TX) RISC workstations, RS/6000 Models 340, 350, 360, 365, and 3CT. As we have described in detail in previous work,[8,15] we use *N*-formyl amino acid amides in our shielding calculations. For example, for isoleucine, we use *N*-formylisoleucine amide:

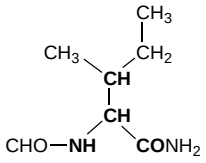

The geometries employed were those obtained by extensively energy minimizing the bond lengths and three atom angles with a steepest descents algorithm, and they represent the geometries present in an Amber force field.[16] *Ab initio* geometry optimization has been studied by us in valine, and the use of geometry optimized structures has only a very small effect on the shieldings observed.[11] We used a locally dense basis set[17] in the coupled Hartree−Fock (CHF) shielding calculations,[13,14] 6-311++G (2d,2p) on the bold atoms shown above, with a 6-311G basis on the other atoms, where the notations refer to the standard basis sets of Pople and co-workers.[18] A detailed study of the basis set dependence of shielding in valine has been reported by us previously (see ref 19 for details).

Results and Discussion

We first consider the principal components of the $^{13}C^\alpha$ shielding tensor for the following *N*-formyl amino acid amides, glycine, alanine, valine, isoleucine, serine, and threonine, to determine the effects of side-chain substitution and conformation on the C^α shielding tensor. In previous work, we have investigated C^α shieldings in glycine, alanine, and valine, but we focused primarily on the isotropic shifts or shieldings, especially in relation to the ability to reproduce ^{13}C chemical shifts in proteins.[1,2] For these three amino acids, we found a good correlation between the experimentally observed ^{13}C shifts and those computed *ab initio*,[1,2,8,10,11,15] which led us to develop methods for the refinement of alanine (ϕ,ψ) and valine (ϕ,ψ,χ) torsion angles in proteins in solution, using these computed shielding surfaces.[3] In addition, once the shielding surfaces are known, it then becomes possible to actually predict, at least for alanine, which ϕ,ψ values are consistent with the experimental chemical shift.[7] For example, for alanine residues in proteins, we have used C^α, C^β, and H^α isotropic shift surfaces to enable the prediction of the experimental ϕ,ψ values to an accuracy (versus the X-ray structure) of about $\pm 10-15°$, using these three parameters.[10] While this difference is quite sizable, the errors in the crystal structures are also approximately this large.[20] In the solid state, H^α shifts are often not accessible, but C^α and C^β shifts should be. Moreover, in smaller peptide systems, it has also recently been shown to be possible to deduce the principal elements of the $^{13}C^\alpha$ shielding tensor, σ_{11}, σ_{22}, and σ_{33}, and then to use these tensor elements to predict ϕ,ψ values in good accord with those deduced from a high-resolution crystal structure.[7] There is thus reason to be optimistic that in the future, *ab initio* computed shielding surfaces, when combined with experimental shielding tensor element measurements, may enable new general approaches to structure determination in proteins, or at the very least, that they should assist in structure refinement, by permitting a rejection of unacceptable solutions (as in the chemical shift refinement of alanine and valine in a *Staphylococcal* nuclease, ref 3). Of course, to be most useful, there should be large shielding differences between helical and sheet structures, and between different side chain conformations. We next consider, therefore, the shielding patterns we observe in six amino acids, which comprise the major ϕ,ψ and χ_1/χ_2 conformations, for a total of 69 shielding surfaces.

C^α in Glycine and Alanine. We first briefly reconsider the two simplest amino acids, glycine and alanine. In the past, these two amino acids have been the topic of investigation by ourselves and by others.[21−24] For example, in early work[8,15] we reported that it was possible to calculate $^{13}C^\alpha$ and C^β shifts of alanine residues in proteins and ^{15}N shifts,[15] and that Ramachandran shielding surfaces correctly predicted the well-

(11) Pearson, J. G.; Le, H.; Sanders, L. K.; Godbout, N.; Havlin, R. H.; Oldfield, E. *J. Am. Chem. Soc.* **1997**, *119*, 11941−11950.
(12) Tjandra, N. T.; Hu, J.-S.; Ottiger, M.; Marquardt, J.; Delaglio, F.; Bax, A. *Experimental NMR Conference*, Orlando, FL, March 26, 1997; Abstracts, p 40.
(13) Wolinski, K.; Hinton, J. F.; Pulay, P. *J. Am. Chem. Soc.* **1990**, *112*, 8251−8260.
(14) Pulay, P.; Wolinski, K.; Hinton, J. F. *The TEXAS Program*; University of Arkansas: Fayetteville, AR, 1991.
(15) de Dios, A. C.; Pearson, J. G.; Oldfield, E. *Science* **1993**, *260*, 1491−1496.
(16) Weiner, P. K.; Kollman, P. A. *J. Comput. Chem.* **1981**, *2*, 287−303. Brooks, B. R.; Bruccoleri, R. E.; Olafson, B. D.; States, D. J.; Swaminathan, S.; Karplus, M. *J. Comput. Chem.* **1983**, *4*, 187−217.
(17) Chestnut, D. B., Moore, K. D. *J. Comput. Chem.* **1989**, *10*, 648−659.
(18) Hehre, W. J.; Radom, L.; Schleyer, P.; Pople, J. A. *Ab Initio Molecular Orbital Theory*; John Wiley and Sons: New York, 1986.
(19) Laws, D. D.; Le, H.; de Dios, A. C.; Havlin, R. H.; Oldfield, E. *J. Am. Chem. Soc*. **1995**, *117*, 9542−9546.
(20) Morris, A. L.; MacArthur, M. W.; Hutchinson, E. G.; Thornton, J. M. *Proteins* **1992**, *12*, 345−364. Thornton, J. M.; Hutchinson, E. G.; Jones, S.; Laskowski, R. A.; MacArthur, M.; Michie, A.; Orengo, C. M.; Rullman, J. A. C.; Kaptein, R. *XVIIth International Conference on Magnetic Resonance in Biological Systems*, Keystone, CO, 1996; Abstracts, p 66.
(21) Asakawa, N.; Kurosu, H.; Ando, I.; Shoji, A.; Ozaki, T. *J. Mol. Struct.* **1994**, *317*, 119−129.
(22) Asakawa, N.; Kurosu, H.; Ando, I. *J. Molec. Struct.* **1994**, *323*, 279−285.
(23) Sulzbach, H. M.; Schleyer, P. v. R.; Schaefer, H. F., III *J. Am. Chem. Soc.* **1995**, *117*, 2632−2637.
(24) Sulzbach, H. M.; Vacek, G.; Schreiner, P. R.; Galbraith, J. M.; Schleyer, P. v. R.; Schaefer, H. F., III *J. Comput. Chem.* **1997**, *18*, 126−138.

known helix-sheet separations for C^{α} and C^{β}.[8,15] However, other workers have reported essentially no correlation between theory and experiment,[21] and attributed the alanine C^{α} shifts seen experimentally to C′ hydrogen bonding,[21] a view that was modified somewhat in later work.[22] Since we have now evaluated ~200 C^{α}/C^{β} shieldings in proteins and found good agreement between theory and experiment, it seems likely that the protein chosen in their studies has either a poor crystal structure, peak misassignments, crystal−solution structural differences, or a combination of these effects, which obfuscates the clear relationships between shift and structure we have found.

In a second series of studies, another group[23,24] has investigated C^{α}, C^{β}, C′, and N^{H} shielding in glycine and alanine model compounds. These workers also noted that good agreement between theory and experiment for C^{α} could not be described only in terms of ϕ and ψ,[24] at variance with our results. They invoked a major change in planarity of the peptide bond, ~30° in helical structures, in order to fit the experimental results on C′.[24] However, this assumption is inconsistent with the experimental *J*-coupling results of Wang and Bax[25] and Hu and Bax,[26] and the $^{15}N-^{1}H$ dipolar coupling results of Tjandra et al.[27] Each of these three experimental studies emphasizes the planar arrangement of the peptide bond, as we have used in our calculations.

Solid-state NMR determinations of N−H dipolar couplings in oriented samples with the separated local field approach also imply the essentially planar nature of the peptide bond.[28] It therefore seems likely that the majority of peptide groups are planar, in actual proteins. Indeed, the results of Sulzbach et al.[24] for C^{α}, where a helix-sheet shielding difference of 7.6 ppm was reported, appear to us to be not unreasonable since the alanine C^{α} shift range can be as much as 10 ppm. The 3−4 ppm experimental helix-sheet shift results quoted by these workers refer simply to "average" helix-sheet $\Delta\delta$ values, with the Spera and Bax $\Delta\delta$ result[29] quoted by these authors being up to 6.8 ppm—very close to their 7.6 ppm helix-sheet separation.

The major problem of course lies with C′, where a *minus* 4.3 ppm helix-sheet separation was calculated,[24] to be compared with the *plus* 4.6 ± 0.3 to 2.1 ± 4.0 range from experiment,[30,31] a problem also encountered by Jiao et al.[32] However, when the effects of hydrogen bonding are taken into account, then good agreement between theory and experiment is obtained.[33] In our work, we thus use planar peptide geometries, for the following reasons: (1) several hundred C^{α} and C^{β} shifts have been correctly predicted by us in proteins using planar peptide geometries; (2) the computed C^{α} shielding tensor elements of alanine are in quite good agreement with experiment, and enable the correct prediction of ϕ,ψ torsions;[7] (3) a chemical shift refined protein structure more closely resembles the x-ray structure than does a solution (NOE) structure, and most importantly, (4) all recent experimental determinations indicate peptide planarity (or up to ≈5° nonplanarity only, refs 25−27).

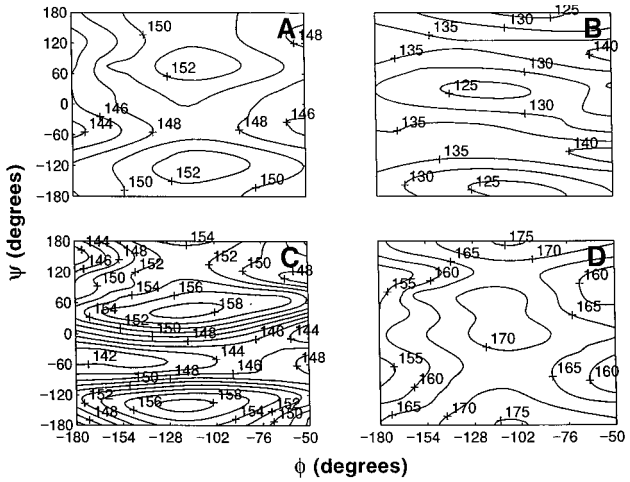

Figure 1. Computed isotropic shieldings and anisotropic shielding tensor elements for $^{13}C^{\alpha}$ in *N*-formylalanine amide obtained by using a Hartree−Fock method with gauge-including atomic orbitals and a locally dense basis set: (A) σ_i; (B) σ_{11}; (C) σ_{22}; and (D) σ_{33}.

We show in Figure 1 full ϕ,ψ Ramachandran shielding surfaces for both the isotropic shielding (σ_i) and anisotropic shielding tensor elements (σ_{11}, σ_{22}, and σ_{33}) for C^{α} of alanine in *N*-formylalanine amide. The general patterns of a more highly shielded extended sheet region ($\phi = -120°$, $\psi = 120°$) over the helical region ($\phi = -60°$, $\psi = -60°$) can be seen for σ_i and each shielding tensor element, and similar results are obtained for glycine at the same ϕ,ψ values, although of course for glycine there are many regions of ϕ,ψ space accessible. The question then arises—How accurate are these shielding tensor surfaces? This question has recently been answered most directly by Heller et al., who measured the C^{α} shielding tensor elements in three tripeptides: gly-*ala-val, ala-*ala-ala, and ala-*ala-ala-hemihydrate,[7] where the * indicates that only the central alanine C^{α} is ^{13}C-labeled. These workers found that, after application of a small scaling factor to the slope of the theory-versus-experiment correlation, due presumably to correlation and perhaps small basis deficiencies, that the shieldings of σ_{11}, σ_{22}, and σ_{33} could be predicted with a root-mean-square error for the nine tensor elements of only ~1 ppm.[7] This is a high degree of precision, and as noted above, has permitted the first successful prediction of ϕ,ψ torsion angles with use of alanine C^{α} shielding tensor elements. Some confidence can, therefore, be placed in the quality of the calculations, since not only are the well-known isotropic chemical shift differences between helical and sheet regions obtained, Table 1, but the individual tensor elements are also quite well reproduced by the calculations.

Now, the cases of glycine and alanine are somewhat unusual in that there is no substitution at C^{β} (or no C^{β} at all), unlike the situation with all of the other 18 common amino acids. Moreover, the C^{α} shielding tensors for glycine and alanine are themselves quite unusual, a fact we did not appreciate until we carried out the calculations on the other amino acids described below. In fact, the overall computed tensor breadths, $|\sigma_{33} - \sigma_{11}|$, for glycine and alanine are some of the largest observed so far, when considering both helical and sheet regions of ϕ,ψ space. For example, as shown in Table 1, we obtain tensor breadths of ~37.4, 32.4 ppm for glycine and ~31.7, 30.7 ppm for alanine in helical and sheet regions of conformational space. There is no obvious distinction between the helical and sheet

(25) Wang, A. C.; Bax, A. *J. Am. Chem. Soc.* **1996**, *118*, 2483−2494.
(26) Hu, J-S., Bax, A. *J. Am. Chem. Soc.* **1997**, *119*, 6360−6368.
(27) Tjandra, N.; Grzesiek, S.; Bax, A. *J. Am. Chem. Soc.* **1996**, *118*, 6264−6272.
(28) Tycko, R.; Stewart, P. L.; Opella, S. J. *J. Am. Chem. Soc.* **1986**, *108*, 5419−5425. Opella, S. J.; Stewart, P. L.; Valentine, K. G. *Q. Rev. Biophys.* **1987**, *19*, 7−49. Chirlian, L. E.; Opella, S. J. *Adv. Magn. Reson.* **1990**, *14*, 183−202. Jelinek, R.; Ramamoorthy, A.; Opella, S. J. *J. Am. Chem. Soc.* **1995**, *117*, 12348−12349.
(29) Spera, S.; Bax, A. *J. Am. Chem. Soc.* **1991**, *113*, 5490−5492.
(30) Kricheldorf, H. R.; Müller, D. *Macromolecules* **1983**, *16*, 615−623.
(31) Wishart, D. S.; Sykes, B. D.; Richards, F. M. *Biochemistry* **1992**, *31*, 1647−1651.
(32) Jiao, D.; Barfield, M.; Hruby, J. M. *J. Am. Chem. Soc.* **1993**, *115*, 10883−10887.
(33) de Dios, A. C.; Oldfield, E. *J. Am. Chem. Soc.* **1994**, *116*, 11485−11488.

Table 1. Summary of Representative Computed C^{α} Shielding Tensor Elements for Several *N*-Formyl Amino Acid Amide Peptide Model Systems[a]

		shieldings (ppm)[b]					orientations	
system	structure	σ_{11}	σ_{22}	σ_{33}	σ_i	$\lvert\sigma_{33}-\sigma_{11}\rvert$	α (deg)[c]	β (deg)[d]
glycine	helix	129.5	156.2	166.9	150.9	37.4	8.7	44.0
	sheet	141.3	150.6	173.7	155.2	32.4	75.8	137.0
alanine	helix	129	147.9	160.7	145.9	31.7	111.3	50.8
	sheet	134.6	152.7	165.3	150.9	30.7	5.8	144.4
valine	helix ($\chi_1 = 180°$)	129.1	132.5	144.1	135.2	15	79.9	69.1
	sheet ($\chi_1 = 180°$)	118.6	145.2	156.0	139.9	37.4	9.6	148.7
	helix ($\chi_1 = -60°$)	120.9	138.6	149.4	136.3	28.5	82.5	68.2
	sheet ($\chi_1 = -60°$)	124.2	144.4	160.6	143.0	36.4	12.9	152.8
	helix ($\chi_1 = 60°$)	128.2	137.8	146.0	137.3	17.8	82.2	63.5
	sheet ($\chi_1 = 60°$)	123.3	152.0	155.2	143.5	31.9	14.7	132.0
isoleucine	helix ($\chi_1 = -60°, \chi_2 = 180°$)	129.1	132.4	145.0	135.5	15.9	51.0	153.8
	sheet ($\chi_1 = -60°, \chi_2 = 180°$)	118.9	145.7	156.1	140.2	37.2	7.9	157.3
	helix ($\chi_1 = -60°, \chi_2 = -60°$)	128.5	138.0	151.6	139.4	23.1	45.1	134.2
	sheet ($\chi_1 = -60°, \chi_2 = -60°$)	119.7	152.1	155.2	142.3	35.5	6.8	161.8
	helix ($\chi_1 = -60°, \chi_2 = 60°$)	126.8	130.6	143.8	133.7	17	31.1	160.7
	sheet ($\chi_1 = -60°, \chi_2 = 60°$)	117.7	144.2	156.2	139.4	38.5	7.2	157.0
serine	helix ($\chi_1 = 74.3°$)	125.7	136.7	149.9	137.4	24.2	95.0	54.2
	sheet ($\chi_1 = 74.3°$)	128.3	148.6	157.3	144.7	29	10.3	154.2
threonine	helix ($\chi_1 = 180°$)	128.7	138.2	147.0	137.9	18.3	72.9	120.2
	sheet ($\chi_1 = 180°$)	125.0	151.4	155.8	144.1	30.8	8.2	164.3
	helix ($\chi_1 = -60°$)	127.7	132.1	141.5	133.8	13.8	62.8	150.4
	sheet ($\chi_1 = -60°$)	121.5	141.6	154.5	139.2	33	2.3	155.7
	helix ($\chi_1 = 60°$)	124.2	139.4	145.9	136.5	21.7	101.6	48.9
	sheet ($\chi_1 = 60°$)	124.9	144.9	157.9	142.6	33	6.8	166.3

[a] The shielding values given are absolute shieldings, computed with the Texas program, as described in the text. [b] The shielding values given are from the computed shielding surfaces. For ease of interpretation, we simply report shielding values at $\phi = -60°$, $\psi = -60°$ ("helix"), and $\phi = -120°$, $\psi = 120°$ ("sheet"). The actual surfaces are available upon request. [c] α is the angle between σ_{11} and the $C^{\alpha}-H$ bond vector. [d] β is the angle between σ_{22} and the $C^{\alpha}-N$ bond vector. Full surfaces and orientations are also available at http://feh.scs.uiuc.edu.

tensor breadths, and the $|\sigma_{33} - \sigma_{11}|$ values observed are quite close to those seen experimentally in the free amino acids, ~40 ppm for glycine[34] and ~34 ppm for alanine.[35] Indeed, as we show in Table 1, the experimentally observed ~5 ppm increased shielding for C^{α} of alanine in a typical "average" sheet versus an α-helical geometry can be seen to be due to a uniform change in σ_{11}, σ_{22}, and σ_{33}, in which all increase their shielding by ~4−7 ppm, Table 1. This results in an overall change in isotropic shift of 5.0 ppm, as would be anticipated from the work of Spera and Bax[29] and Wishart et al.[31] We show in Figure 2 a "stick-diagram" illustrating the results of Table 1, for typical helix-sheet geometries, in each of the amino-acids and conformers we have investigated.

The results given in Table 1 and Figures 1 and 2 show that in most cases for glycine and alanine there is a uniform increase in shielding for each tensor element upon helix → sheet transition, and that there are only minor changes in $|\sigma_{33} - \sigma_{11}|$. This, however, is not the pattern that emerges upon inspection of numerous β-substituted systems, as we describe below.

C^{α} in Valine and Isoleucine. We next investigated C^{α} shielding in valine and isoleucine. For valine, we studied all three rotomers ($\chi_1 = 180°$, $-60°$, $60°$), while for isoleucine we studied the two most abundant conformers[36] ($\chi_1 = -60°$, $\chi_2 = 180°$; $\chi_1 = -60°$, $\chi_2 = -60°$) along with the third $\chi_1 = -60°$ conformer, in which $\chi_2 = 60°$. We show in Figure 3 the σ_i, σ_{11}, σ_{22}, and σ_{33} Ramachandran (ϕ,ψ) shielding surfaces for valine at the most popular $\chi_1 = 180°$ conformation, and in Figure 4 the same series of surfaces for valine in the second most populous[36] $\chi_1 = -60°$ conformation. Similar surfaces were computed for $\chi_1 = 60°$, and typical values for σ_i, σ_{11}, σ_{22}, σ_{33}, $|\sigma_{33} - \sigma_{11}|$, and $|\sigma_{22} - \sigma_{11}|$ for valine and isoleucine in representative helical and sheet geometries are tabulated in Table 1 and shown graphically in Figure 2.

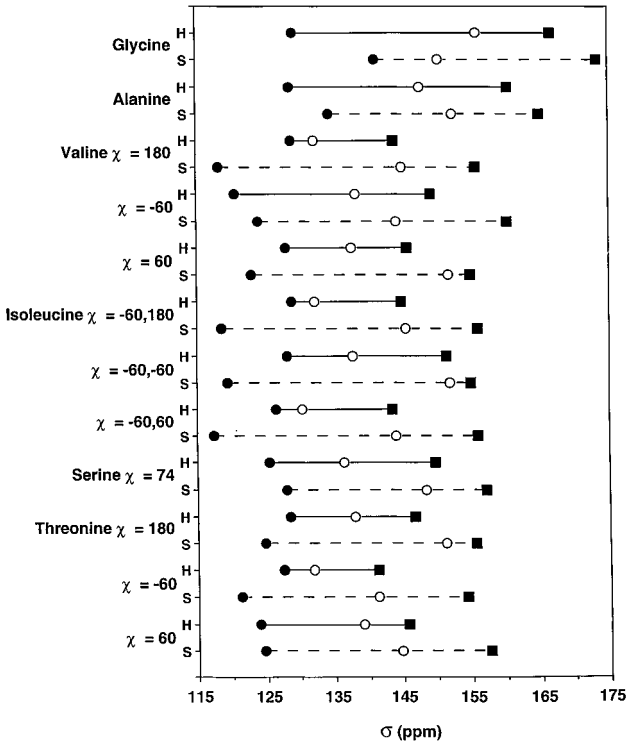

Figure 2. Diagram showing the shielding tensor elements, σ_{ii}, for each system investigated: ●, σ_{11}; ○, σ_{22}, and ■, σ_{33}. The solid lines join the helical data sets, the broken lines join the sheet data sets.

Upon C^{β} substitution, there are major changes in shielding tensor properties observed between helical and sheet geometries, a trend which carries over to the other C^{β} substituted systems

(34) Haberkorn, R. A.; Stark, R. E.; van Willigen, H.; Griffin, R. G. *J. Am. Chem. Soc.* **1981**, *103*, 2534−2539.
(35) Naito, A.; Ganapathy, S.; Akasaka, K.; McDowell, C. A. *J. Chem. Phys.* **1981**, *74*, 3190−3197.
(36) Ponder, J. W.; Richards, F. M. *J. Mol. Biol.* **1987**, *193*, 775−791.

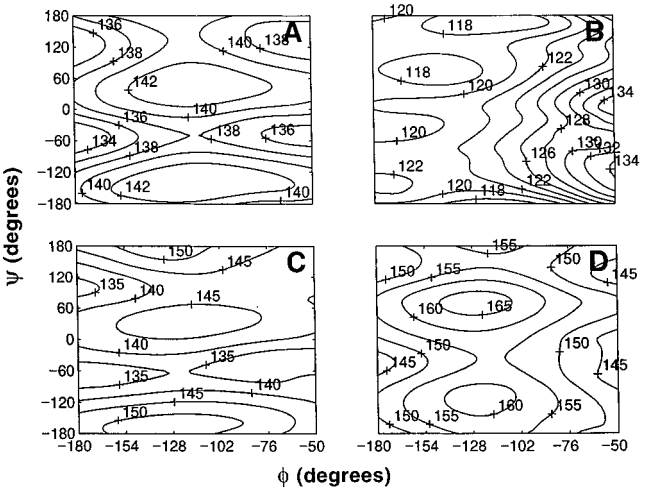

Figure 3. Computed isotropic shieldings and anisotropic shielding tensor elements for $^{13}C^{\alpha}$ in *N*-formylvaline amide ($\chi_1 = 180°$) obtained by using a Hartree−Fock method with gauge-including orbitals and a locally dense basis set: (A) σ_i; (B) σ_{11}; (C) σ_{22}; and (D) σ_{33}.

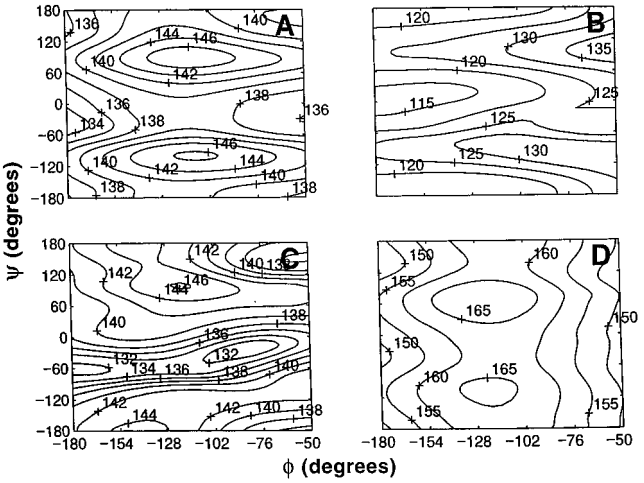

Figure 4. Computed isotropic shieldings and anisotropic shielding tensor elements for $^{13}C^{\alpha}$ in *N*-formylvaline amide ($\chi_1 = -60°$) obtained by using a Hartree−Fock method with gauge-including orbitals and a locally dense basis set: (A) σ_i; (B) σ_{11}; (C) σ_{22}; and (D) σ_{33}.

as well (see below). In particular, it is clear that, in general, the C^{α} shielding tensors for the helical residues have spans of only about two-thirds of those observed for sheet geometries, as summarized in Table 2. When additional results for serine and threonine are included, we find on average that $|\sigma_{33} - \sigma_{11}|$ for helical residues is ∼22 ppm, while $|\sigma_{33} - \sigma_{11}|$ for the sheet residues is ∼34 ppm, Table 2. And unlike the situation seen with alanine, the individual tensor elements move in a more varied pattern on helix → sheet conversion. For example, for valine ($\chi_1 = 180°$), σ_{11} becomes deshielded by 10.5 ppm, while σ_{22} and σ_{33} become shielded by 12.7 and 11.9 ppm, respectively.

Interestingly, we also observe on average the ∼5 ppm increase in shielding of sheet over helical fragments for the isotropic shielding, as shown in Table 2, as expected based on previous experimental chemical shift measurements.[29−31] However, unlike alanine, the changes in the individual tensor elements vary widely between helical and sheet structures.

These observations are important since they suggest a route to structure determination, or at least refinement, may exist via experimental determination of the individual shielding tensor elements, an approach which should find particular utility in investigating the structures of peptides and proteins in the solid

Table 2. Summary of Overall Computed $^{13}C^{\alpha}$ NMR Shielding Tensor Breadths and Isotropic Shielding Differences for Various *N*-Formyl Amino Acid Amide Peptide Model Systems in Helical and Sheet Geometries

system	$\lvert\sigma_{33}$-$\sigma_{11}\rvert$, ppm: helical	$\lvert\sigma_{33}$-$\sigma_{11}\rvert$, ppm: sheet	$-(\sigma_i^{helix} - \sigma_i^{sheet})$,[a] ppm
glycine	37.4	32.4	4.3
alanine	31.7	30.7	5.0
valine ($\chi_1 = 180°$)	15	37.4	4.7
($\chi_1 = -60°$)	28.5	36.4	6.7
($\chi_1 = 60°$)	17.8	31.9	6.2
isoleucine ($\chi_1 = -60°$, $\chi_2 = 180°$)	15.9	37.2	4.7
($\chi_1 = -60°$, $\chi_2 = -60°$)	23.1	35.5	2.9
($\chi_1 = -60°$, $\chi_2 = 60°$)	17	38.5	5.7
serine ($\chi_1 = 74.3°$)	24.2	29	7.3
threonine ($\chi_1 = 180°$)	18.3	30.8	6.2
($\chi_1 = -60°$)	13.8	33	5.4
($\chi_1 = 60°$)	21.7	33	6.1
av value for C^{β}-substituted residues	∼22	∼34	∼5.4

[a] The C^{α} in helices are on average about 5 ppm downfield from the sheet residues.

state. For example, for valine, measurement of the isotropic shift permits a distinction between helical (σ_i = 135.2, 136.3, 137.3 ppm) and sheet (σ_i = 139.9, 143, 143.5 ppm) residues. The sheet residues can then be further differentiated since the σ_i for $\chi_1 = 180°$ is unique (139.9 ppm), and $|\sigma_{33} - \sigma_{11}|$ and $|\sigma_{22} - \sigma_{11}|$ are 36.4, 20.2 ppm ($\chi_1 = -60°$) and 31.9, 28.7 ppm ($\chi_1 = 60°$). Similarly, for the helical sites, the −60° conformer has a uniquely broad $|\sigma_{33} - \sigma_{11}|$ of 28.5 ppm. This effect can be traced to an anomalously large paramagnetic shift for σ_{11}. In addition, the −60° conformer has the most shielded σ_{33} among the helical geometries (see Table 1). This is unusual, and it is likely associated with the relatively infrequent occurrence of α-helices containing valines with $\chi_1 = -60°$, due to the high energy of this state. The 180°, 60° conformers have very similar $|\sigma_{33} - \sigma_{11}|$ and $|\sigma_{22} - \sigma_{11}|$ and are unlikely to be readily differentiated experimentally. However, valines having $\chi_1 = 60°$ in a helix are virtually unknown. Of course, with the addition of χ_1, there is an additional degree of freedom, and we do not suggest that the transformation $(\sigma_{11},\sigma_{22},\sigma_{33}) \rightarrow (\phi,\psi,\chi_1)$ can be routinely made solely based on a C^{α} tensor measurement. In principle, χ_1 is also a free variable, although based on recent work on valine shielding calculations[11] it is clear that only small variations in χ_1 are permissible. Rather, the results of Table 1 strongly suggest that the availability of C^{α} shielding tensor elements, when combined with other information, should facilitate the refinement of solid-state structures. Such other information could include, e.g., distance information, as well as information on C^{β}, C^{γ_1}, C^{γ_2} shifts, which in many cases are also sensitive to ϕ,ψ,χ_1.[11]

As expected, the results for isoleucine closely track those seen with valine, since C^{δ} is quite remote, although γ-gauche contributions to overall shielding can be expected in some situations. As with valine, the overall results for isoleucine indicate a large increase in tensor breadth for sheet versus helical geometries. In addition, it is interesting to note that the orientation of the C^{α} shielding tensor for isoleucine is similar to that of valine. For the most populous isoleucine conformation ($\chi_1 = -60°$, $\chi_2 = 180°$), the sheet tensor is more than twice as broad as the helical tensor, Table 1, and is accompanied by a ∼4.7 ppm increase in overall isotropic shielding. For the second most populous conformation ($\chi_1 = -60°$, $\chi_2 = -60°$), the sheet tensor is very similar to the −60°, 180° sheet tensor, but the helical conformer increases its breadth. Interestingly, the isotropic shielding for the −60°, 180° sheet is almost the same

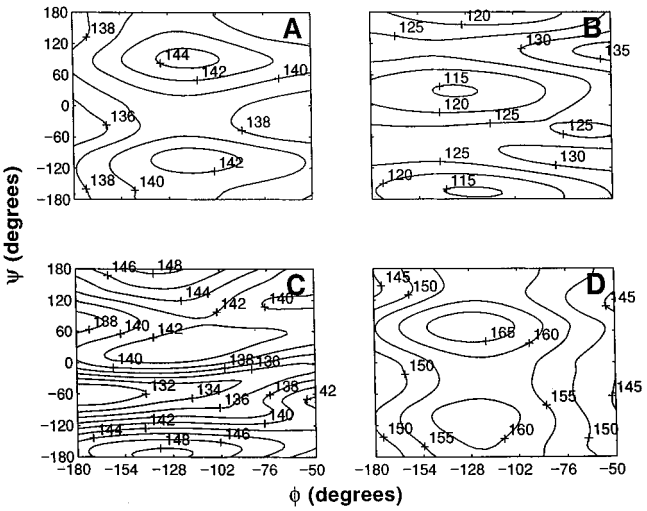

Figure 5. Computed isotropic shieldings and anisotropic shielding tensor elements for $^{13}C^{\alpha}$ in *N*-formylthreonine amide ($\chi_1 = 60°$) computed with a Hartree−Fock method with gauge-including atomic orbitals and a locally dense basis set: (A) σ_i; (B) σ_{11}; (C) σ_{22}; and (D) σ_{33}.

as that for the −60°, −60° helix, Table 1, but these two possibilities can be differentiated on the basis of the large differences in $|\sigma_{33} - \sigma_{11}|$ and $|\sigma_{22} - \sigma_{11}|$, Tables 1 and 2. The $\chi_1 = -60°$, $\chi_2 = 60°$ results are very similar to those found for the most abundant conformer, Table 1, but the C^{β} results are very different, and in addition this conformer is of very low abundance in proteins.[36]

Serine and Threonine. We next consider the cases of the two hydroxy amino acids, serine and threonine, which both have O-substitutions on C^{β}. We show in Figure 5 a representative set of shielding surfaces for threonine with $\chi_1 = 60°$. In each case, the C^{α} tensor breadth is much smaller for the helical geometries than for the sheet structures, Table 2.

For threonine, unlike valine, the isotropic shieldings do not permit a complete distinction between helical and sheet structures, since the $\chi_1 = 180°$ helix and $\chi_1 = -60°$ sheet shieldings are so similar. However, for the −60° sheet, $|\sigma_{33} - \sigma_{11}|$ is 33 ppm, while for the 180° helix, $|\sigma_{33} - \sigma_{11}| = 18.3$ ppm, which permits the formal differentiation between helices and sheets (and the $\chi_1 = 180°$ in threonine are very rare in any case). Assignment to the $\chi_1 = \pm 60°$ conformers in helical and sheet threonines can thus be made, since the 180° conformer for threonine is energetically very unlikely.[36] For serine, we have carried out a less complete series of shielding investigations. Nevertheless, we find similar results to those obtained with the other β-substituted amino acids, with a 7.3 ppm increase in shielding for the sheet vs helical structures, and a smaller overall tensor breadth for the helical regions, Tables 1 and 2.

***β*-Carbon Shielding Tensors.** We have also evaluated the C^{β} shielding tensors for alanine, valine, isoleucine, serine, and threonine. Results are given in Table 4. The C^{β} results are more varied than those with C^{α}, which is not unanticipated given that there are major electronic structural changes involved at the site of substitution. In most cases for popular side chain conformations, our results show rather little difference between helical and sheet tensor breadths, and in general the C^{β} tensors more closely approach axial asymmetry. For alanine, the C^{β} tensor breadths are ∼33−38 ppm for typical helical, sheet geometries. For the two most populous threonines, both tensors are about 40 ppm broad. For isoleucine, Figure 6, the C^{β} tensor breadths are all small (as with valine, Table 4) and only ϕ,ψ sensitive for the second most populous conformer. These results indicate that C^{β} tensor elements are less likely to be useful in structural analysis than C^{α}, although they will generally be complementary. For example, the $\chi_1 = +60°$ C^{β} tensor breadth in threonine, Figure 7, is 10 ppm narrower than that of the $\chi_1 = 180°$ conformer, permitting a validation of conclusions which can be drawn from C^{α} results, Table 1. Interestingly, the extreme breadth of the C^{β} tensor in all threonines is very similar to that observed in the free amino acid, where full (single-crystal) tensors have been determined previously.[37] Results for C^{β} thus often map the free amino acid results, and are dominated more by the type of C^{β} substitution, rather than ϕ,ψ effects.

Table 3. Summary of Computed Values for $^{13}C^{\alpha}|\sigma_{22} - \sigma_{11}|$ for Various *N*-Formyl Amino Acid Amide Peptide Model Systems

system		$\lvert\sigma_{22} - \sigma_{11}\rvert$, ppm helix	sheet
glycine		26.7	9.3
alanine		18.9	18.1
valine	($\chi_1 = 180°$)	3.4	26.6
	($\chi_1 = -60°$)	17.7	20.2
	($\chi_1 = 60°$)	9.6	28.7
isoleucine	($\chi_1 = -60°$, $\chi_2 = 180°$)	3.3	26.8
	($\chi_1 = -60°$, $\chi_2 = -60°$)	9.5	32.4
	($\chi_1 = -60°$, $\chi_2 = 60°$)	3.8	26.5
serine	($\chi_1 = 74.3°$)	11	20.3
threonine	($\chi_1 = 180°$)	9.5	26.4
	($\chi_1 = -60°$)	4.4	20.1
	($\chi_1 = 60°$)	15.2	20
av value for C^{β}-substituted residues		∼9	∼25

We should also note that these examples likely represent a "worst case" scenario. For example, for alanine, the calculations do in fact show a wide range of shifts in the sheet region, and the overall breadth we have taken is just applicable to one point. If σ_{11}, σ_{22}, and σ_{33} shielding tensor elements were all available, it is not unlikely that an estimate of ϕ,ψ might still be made, as with C^{α},[7] and indeed by using Bayesian probability, all six tensor elements can be combined to provide an accurate ϕ,ψ solution.

The Tensor Orientations. We have also investigated the C^{α} and C^{β} tensor orientations for each amino acid conformer in both helical and sheet regions of ϕ,ψ space. Some typical results for valine are illustrated in Figure 8. Of particular interest is the pronounced change in orientation of the C^{α} tensor between helical and sheet regions, parts A and B in Figures 8A and 8B. This is somewhat surprising, since there are no covalent bonding changes. However, the C^{α} tensor in amino acids has no immediately obvious interaction governing shielding, or any obvious symmetry axis,[22,37] so the large changes in tensor breadth and orientation upon rotation of two attached peptide planes is not unreasonable, and knowledge of such tensor orientations can be expected to be of help in analyzing, e.g., ^{13}C NMR spectra of oriented samples. A quantitative description of the C^{α} tensor orientation is given in Table 1 in which we define angles of α, the angle between σ_{11} and the $C^{\alpha}-H$ vector, and β, the angle between σ_{22} and the $C^{\alpha}-N$ vector. The orientation of the most deshielded tensor element, σ_{11}, with respect to the $C^{\alpha}-H$ bond vector (α), varies somewhat between helical amino acids (except glycine, which is omitted from consideration here), Table 1, being centered at about 82°. In the sheet residues, however, α is centered at about 8°. This orientational information should be of use in analyzing solution and solid-state spectra, and is available electronically.[38] Most helical C^{α} tensors have similar orientations when compared at

(37) Janes, N.; Ganapathy, S.; Oldfield, E. *J. Magn. Reson.* **1983**, *54*, 111−121.

(38) Havlin, R. H.; Le, H.; Laws, D. D.; deDios, A. C.; Pearson, J. G.; Oldfield, E. *The Web* **1997**, http://feh.scs.uiuc.edu.

Table 4. Summary of Representative Computed C^{β} Shielding Tensor Elements for Several *N*-Formyl Amino Acid Amide Peptide Model Systems[a]

		shieldings (ppm)[b]				
system	structure	σ_{11}	σ_{22}	σ_{33}	σ_i	$\lvert\sigma_{33}-\sigma_{11}\rvert$
alanine	helix	161.7	170.8	194.2	175.5	32.5
	sheet	154.8	169.2	193.2	172.4	38.4
valine	helix ($\chi_1 = 180°$)	159.9	165.2	174.6	166.6	14.7
	sheet ($\chi_1 = 180°$)	155.5	159.5	176.4	163.8	20.9
	helix ($\chi_1 = -60°$)	166.9	168.5	175.1	170.1	8.2
	sheet ($\chi_1 = -60°$)	159.4	164.1	173.9	165.8	14.5
	helix ($\chi_1 = 60°$)	161.7	171.2	175.3	169.4	13.6
	sheet ($\chi_1 = 60°$)	154.3	166.5	176.8	165.9	22.5
isoleucine	helix ($\chi_1 = -60°$, $\chi_2 = 180°$)	150.4	158.2	169.8	159.5	19.4
	sheet ($\chi_1 = -60°$, $\chi_2 = 180°$)	146.1	155.7	168.7	156.8	22.6
	helix ($\chi_1 = -60°$, $\chi_2 = -60°$)	156.6	162.5	169.2	162.8	12.6
	sheet ($\chi_1 = -60°$, $\chi_2 = -60°$)	149.1	159.6	170.5	159.7	21.4
	helix ($\chi_1 = -60°$, $\chi_2 = 60°$)	159.1	161.5	166.7	162.5	7.6
	sheet ($\chi_1 = -60°$, $\chi_2 = 60°$)	158.3	162.2	166.6	162.3	8.3
serine	helix ($\chi_1 = 74.3°$)	118.4	125.6	160.5	134.8	42.1
	sheet ($\chi_1 = 74.3°$)	117.7	124.3	152.2	131.4	34.5
threonine	helix ($\chi_1 = 180°$)	112.4	121.5	163.0	132.3	48.6
	sheet ($\chi_1 = 180°$)	109.2	117.7	162.5	129.8	53.3
	helix ($\chi_1 = -60°$)	113.7	122.6	156.2	130.8	42.5
	sheet ($\chi_1 = -60°$)	113.3	122.9	153.6	129.9	40.3
	helix ($\chi_1 = 60°$)	115.9	122.1	158.1	132.0	42.2
	sheet ($\chi_1 = 60°$)	114.9	122.4	151.9	129.7	37

[a] The shielding values given are absolute shieldings, computed with the Texas program, as described in the text. [b] The shielding values given are from the computed shielding surfaces. For ease of interpretation, we simply report shielding values at $\phi = -60°$, $\psi = -60°$ ("helix") and $\phi = -120°$, $\psi = 120°$ ("sheet"). The actual surfaces are available upon request.

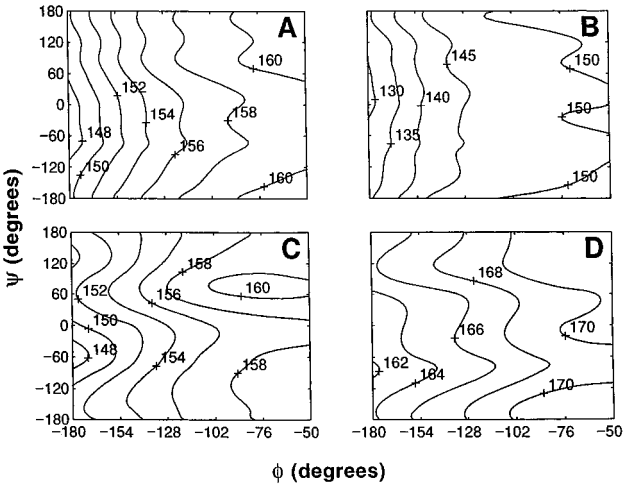

Figure 6. Computed isotropic shieldings and anisotropic shielding tensor elements for $^{13}C^{\beta}$ in *N*-formylisoleucine amide ($\chi_1 = -60°$; $\chi_2 = 180°$; the most abundant conformer) obtained by using a Hartree−Fock method with gauge-including atomic orbitals and a locally dense basis set. (A) σ_i; (B) σ_{11}; (C) σ_{22}; and (D) σ_{33}.

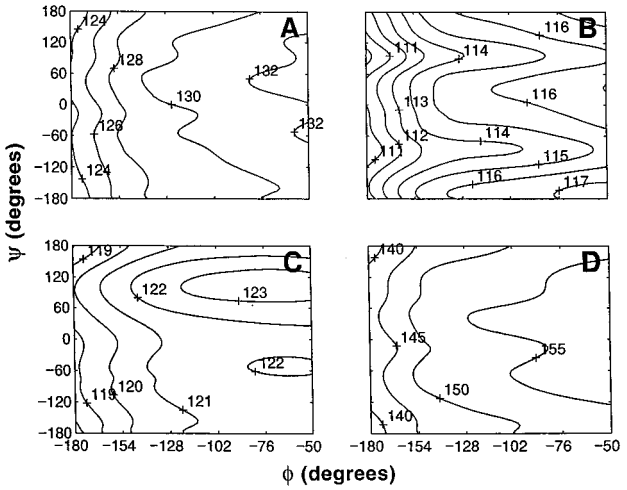

Figure 7. Computed isotropic shieldings and anisotropic shielding tensor elements for $^{13}C^{\beta}$ in *N*-formylthreonine amide ($\chi_1 = 60°$, the most abundant conformer) obtained by using a Hartree−Fock method with gauge-including atomic orbitals and a locally dense basis set: (A) σ_i; (B) σ_{11}; (C) σ_{22}; and (D) σ_{33}.

similar geometries, although glycine and alanine do vary, as shown in Figure 9.

For C^{β}, the similarities in the helical/sheet C^{β} tensor breadths are mirrored in the similarities in tensor orientations, and we show results for the most populous threonine and isoleucine conformers in Figure 10. Clearly, the largest effects on both the breadth and the orientation of C^{α} and C^{β} shielding tensors are due to the most local changes. For C^{α}, the four attached atoms are the same for all β-branched amino acids, and in most cases we expect the same basic increased overall shielding and shielding breadth for sheet versus helical residues, and the orientational changes seen in Figure 8. For the β-carbons, however, there are also different chemical substitutions between C^{β}s, and these tend to dominate the shift anisotropies and tensor orientations. For example, the threonine C^{β} has an extremely broad tensor, ∼40−50 ppm—essentially that seen in the free zwitterionic amino acid,[37] due to OH and Me substitution at C^{β}, while the isoleucine C^{β} breadth is only one half this value, and notably, these tensor orientations do not change appreciably between helical and sheet conformers. Again, as with C^{α}, the full shielding tensor surfaces for all C^{β}, and their orientations, are available electronically.[38]

Conclusions

The results we have described above are of interest for several reasons. First, they represent the first detailed high level theoretical calculations of amino acid shielding in a sizable number of aliphatic and hydroxyl-containing amino acids, in different conformational states: glycine, alanine, valine ($\chi_1 =$

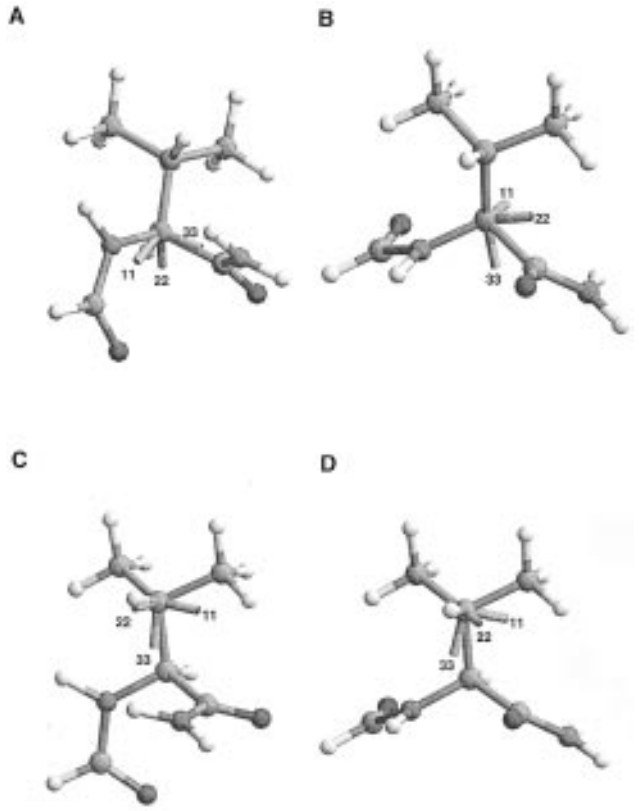

Figure 8. Orientations of the principal components of the $^{13}C^{\alpha}$ and C^{β} shielding tensor for valine ($\chi_1 = 180°$) in helical and sheet geometries: (A) $^{13}C^{\alpha}$, helix; (B) C^{α}, sheet; (C) C^{β}, helix, and (D) C^{β}, sheet.

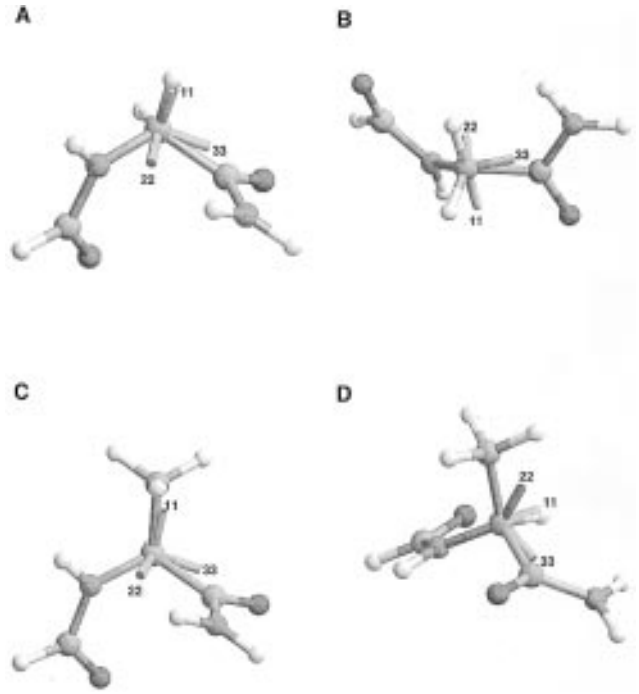

Figure 9. Orientations of the principal components of the $^{13}C^{\alpha}$ shielding tensor elements for glycine and alanine in helical and sheet geometries: (A) glycine helix; (B) glycine, sheet; (C) alanine, helix; and (D) alanine, sheet.

180°, −60°, 60°), isoleucine (all three $\chi_1 = -60°$ forms), serine ($\chi_1 = 74.3°$), and threonine ($\chi_1 = 180°$, −60°, 60°). Second, in each system, we find that C^{α} in sheet structures are on average about 4−5 ppm more shielded than in helical structures, consistent with previous experimental results.[29−31] Third, we find that, on average, the overall breadths of the $^{13}C^{\alpha}$ shielding tensors in sheet residues are about 50% larger than the values computed for helical residues, an unexpected result. Fourth, we find that the C^{α} shielding tensors for the simplest amino acids, glycine and alanine, are atypical. In particular, the helical tensor breadths are very large (≳35 ppm), and are in fact close to the free amino acid tensor breadths (∼35−40 ppm). Moreover, with alanine the tensor elements (σ_{11}, σ_{22}, σ_{33}) all become shielded by about the same amount on helix → sheet conversion, an effect not seen with the β-substituted amino acids. Fifth, our results show that it should be possible to make estimates of ϕ,ψ and χ_1 in many cases, by using both the isotropic and anisotropic components of the shielding tensor. Such shielding tensor surfaces have already permitted the successful prediction of alanine ϕ,ψ values in a peptide from a tensor which changes little between helical and sheet regions.[7] The much larger changes in C^{α} shielding seen between helical and sheet regions in the β-substituted amino acids should thus enable, if not in all cases accurate ϕ,ψ,χ_1 predictions, then at least refinement. Sixth, the availability of numerous tensor orientations is of interest, not only from the standpoint of their similarity between related structures, but knowledge of the full tensors and their orientations should be of use in analyzing results from oriented systems, as well as facilitating the analysis of a variety of angular correlation experiments. And finally, seventh, the results for the C^{β} tensors show large differences between amino acids (due to different chemical substitutions). However, the helix-sheet differences are much smaller than for C^{α} in the most popular conformations, although in some cases they may still provide additional probes of χ_1.

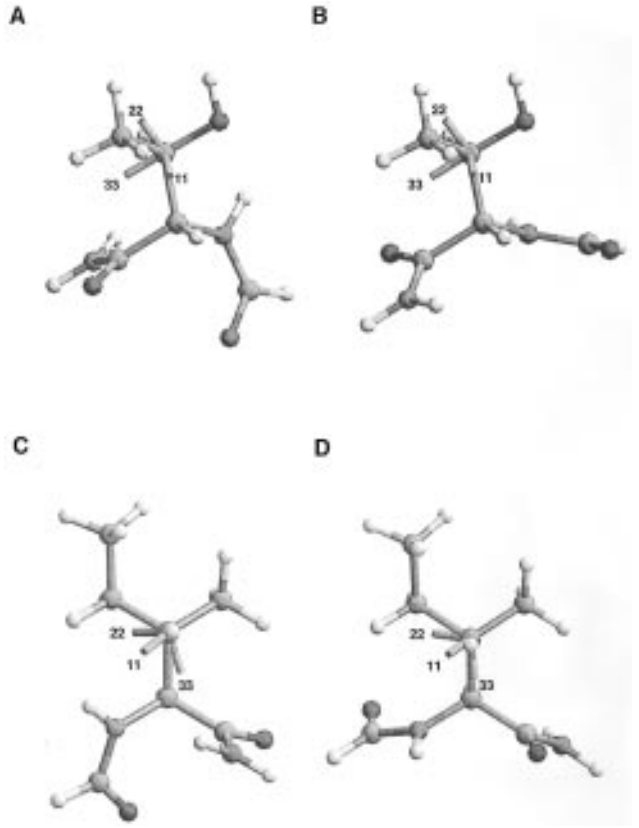

Figure 10. Orientations of the principal components of the $^{13}C^{\beta}$ shielding tensor elements for threonine ($\chi_1 = -60°$) and isoleucine ($\chi_1 = -60°$, $\chi_2 = 180°$) in helical and sheet geometries: (A) threonine, helix; (B) threonine, sheet; (C) isoleucine, helix; (D), isoleucine, sheet.

JA971796D